Comparison of Heat- and Pressure-Induced Unfolding of Ribonuclease A: The Critical Role of Phe46 Which Appears To Belong to a New Hydrophobic Chain-Folding Initiation Site†

Eri Chatani,‡ Kazuhiko Nonomura,‡ Rikimaru Hayashi,*,‡ Claude Balny,§ and Reinhard Lange§

Division of Applied Life Sciences, Graduate School of Agriculture, Kyoto University, Sakyo-ku, Kyoto 606-8502, Japan, and INSERM U128, IFR 24, 1919 Route de Mende (CNRS), F-34293 Montpellier Cedex 5, France

Received June 29, 2001; Revised Manuscript Received February 4, 2002

ABSTRACT: To clarify the structural role of Phe46 inside the hydrophobic core of bovine pancreatic ribonuclease A (RNase A), thermal and pressure unfolding of wild-type RNase A and three mutant forms (F46V, F46E, and F46K) were analyzed by fourth-derivative UV absorbance spectroscopy. All the mutants, as well as the wild type, exhibited a two-state transition during both thermal and pressure unfolding, and both T_m and P_m decreased markedly when Phe46 was replaced with valine, glutamic acid, or lysine. The strongest effect was on the F46K mutant and the weakest on F46V. Both unfolding processes produced identical blue shifts in the fourth-derivative spectra, indicating that the tyrosine residues are similarly exposed in the temperature- and pressure-induced unfolded states. A comparison of Gibbs free energies determined from the pressure and temperature unfoldings, however, gave $\Delta G_p/\Delta G_t$ ratios (r) of 1.7 for the wild type and 0.92 ± 0.03 for the mutants. Furthermore, the ΔV value for each mutant was larger than that for the wild type. CD spectra and activity measurements showed no obvious major structural differences in the folded state, indicating that the structures of the Phe46 mutants and wild type differ in the unfolded state. We propose a model in which Phe46 stabilizes the hydrophobic core at the boundary between two structural domains. Mutation of Phe46 decreases protein stability by weakening the unfolding cooperativity between these domains. This essential function of Phe46 in RNase A stability indicates that it belongs to a chain-folding initiation site.

New understanding of the molecular origins of diseases induced by prions or prion-like proteins has stimulated renewed interest in the mechanisms of protein folding and unfolding. The principles that underlie the formation of stable conformations, however, are still not clear, and there have been extensive studies of model proteins. Bovine pancreatic ribonuclease A (RNase A, EC 3.1.27.5) (*1*, *2*) is a representative well-characterized protein. It consists of a single polypeptide chain with four disulfide bonds. Efforts have been made to trap kinetic folding/unfolding intermediates by stopped-flow spectroscopic or NMR analyses (*3*−*9*), by the use of mutants which are structurally analogous to hypothetical folding intermediates (*10*−*15*), and by chemically blocking free cysteine residues during refolding from the unfolded state, in which the sulfhydryl groups are reduced (*16*−*19*). Partially ordered structures [also called "chain-folding initiation sites" (CFIS) (*3*, *17*, *20*−*26*)] of RNase A have been identified within the initial folding steps needed for formation of the native conformation. One sequence, spanning residues 106−118 (*27*−*29*), forms a partial tertiary structure, in which hydrophobic interactions and side chain packing interactions have a major role in the folding process (*9*, *30*−*32*). The significance of hydrophobic residues other than those within this CFIS of residues 106−118 (CFIS 106−118), however, has yet to be fully evaluated. To better understand the chain folding events, we examined other RNase A structural motifs which may serve as hydrophobic CFIS elements.

Because of its location and hydrophobic interactions, Phe46 is a good candidate for another CFIS constituent. This residue is well-conserved among mammalian ribonucleases. It is located in the middle of the first β-sheet (residues 43−48). Its side chain is directed to the opposite side of the CFIS 106−118 residues, and it faces Met29 and Met30 which also are well-conserved in mammalian ribonucleases. These observations suggest that Phe46 functions to maintain conformational stability. To assess this possibility, we constructed three variant forms (F46V, F46E, and F46K) and compared their conformational stabilities with the stability of the wild-type protein.

The findings of Torrent et al. for CFIS 106−118 suggest that the heat- and pressure-induced unfolded conformations are identical with respect to energy (*28*), but closer inspection

† This work was supported in part by grants from the Institut National de la Santé et de la Recherche Médicale and the Japan Society for the Promotion of Science (JSPS), a Grant-in-Aid for Scientific Research from the Ministry of Education, Science, Sports, and Culture of Japan, and a grant from the Japan Society for the Promotion of Science (JSPS) to E.C. Part of the DSC data was taken from the Master's Thesis (1999) of K.N., a part of whose work was guided by Drs. Hiroshi Ueno (present address, Department of Food Science, Nara Women's University, Kitauoyanishimachi, Nara 630-8506, Japan) and Naoki Tanimizu [present address, Kanagawa Academy of Science and Technology (KAST), 907 Nogawa, Miyamae-ku, Kawasaki, Kanagawa 216-0001, Japan] in addition to the supervising professor, R.H.

* To whom correspondence should be addressed. Phone: +81-75-753-6110. Fax: +81-75-753-6128. E-mail: hayashi@kais.kyoto-u.ac.jp.

‡ Kyoto University.

§ INSERM U128, IFR 24.

10.1021/bi011365e CCC: $22.00
Published on Web 03/15/2002

by high-pressure FTIR suggests that this similarity is coincidental (*29*). To determine whether the conclusions of the CFIS 106−118 study can be generalized, it was necessary to compare the heat- and pressure-induced unfolding of the Phe46 mutants.

Pressure is a thermodynamic perturbant often used in folding and unfolding studies (*33*−*35*). The reason for the interest in high pressure (as compared to heat or chemical denaturants) is that it is a mild, often reversible perturbant which weakens the cooperativity in protein unfolding (*36*) by specifically affecting electrostatic and hydrophobic interactions. In principle, this should facilitate the trapping of thermodynamically stable intermediates which might otherwise escape detection. Panick and Winter (*37*) reported that the folding funnel (*38*) for thermally induced unfolding has a relatively smooth topology and that for pressure-induced unfolding a rough one. Consistent with this is the finding of a multistep, pressure−unfolding curve for carboxypeptidase Y and that, during unfolding, a molten globule-like folding intermediate is present, whereas thermal unfolding is characterized by a two-state transition (*39*). Pressure also provides useful information about volume changes (ΔV) during unfolding.

We used fourth-derivative UV spectroscopy to monitor the thermal- and pressure-induced unfoldings of the wild type and three Phe46 mutant enzymes, a technique which reflects the increase in the polarity of the microenvironment of the six RNase A tyrosine residues due to increased exposure to water on protein unfolding. Furthermore, CD and DSC were used to obtain additional information about secondary and tertiary structural changes. Two questions are addressed. (1) What is the role of the hydrophobic interactions of Phe46? (2) Do heat and pressure produce different unfolding intermediates? Our findings led us to establish a structural unfolding model of RNase A. They also suggest that RNase A has two distinct domains.

MATERIALS AND METHODS

Materials. A DNA plasmid, obtained as described elsewhere (*40*), was used to express mutant RNase A. *Escherichia coli* strain BL21(DE3) [F^- *ompT hsdS*$_B$(r_B-m_B-) *gal dcm* (DE3)] was purchased from Novagen (Milwaukee, WI). Oligonucleotides were synthesized by Japan Bioservice (Saitama, Japan). The Quickchange Site-Directed Mutagenesis Kit was from Stratagene Cloning Systems (La Jolla, CA), and the ABI Prism Big Dye Terminator Cycle Sequencing Ready Reaction DNA Sequencing Kit was from Perkin-Elmer. The IPTG and DTT used in the *E. coli* expression system were from Nacalai Tesque (Kyoto, Japan). Commercial RNase A from Sigma (type I-A, St. Louis, MO) that had been further purified in an FPLC apparatus equipped with a Mono S HR 5/5 column (Pharmacia, Piscataway, NJ) was the control. C>p[1] was purchased from Nacalai Tesque.

Mutagenesis. Mutant plasmids used to express Phe46 mutant RNase A (F46V, F46A, F46E, and F46K) were constructed with a Quickchange Site-Directed Mutagenesis Kit. The primer sequences designated to replace the Phe46 codon with other amino acid codons were 5′-AGCCAGTTAACACA GTG (for Val)/GCT (for Ala)/GAG (for Glu)/AAG (for Lys) GTCCACGAGAGT-3′ and 5′-ACTCTCGTGGAC CAC (for Val)/AGC (for Ala)/CTC (for Glu)/CTT (for Lys) TGTGTTAACTGGCT-3′. Mutations introduced into the plasmid were confirmed by DNA sequencing in an ABI Prism Applied Biosystems 310 Genetic Analyzer (Perkin-Elmer) by means of dideoxy terminator sequencing. Each mutated plasmid then was introduced into the BL21(DE3) strain. Transformed cell selection was based on ampicillin resistance.

Production and Purification of the Wild Type and RNase A Mutants. Proteins were expressed by the method of Dodge and Scheraga (*14*) with the following minor modifications. The transformed strain was incubated at 37 °C in 1 L of LB medium (1% tryptone, 0.5% yeast extract, and 1% NaCl, with the pH adjusted to 7.0) containing 50 μg/mL ampicillin until the cells had grown to an absorbance of 0.8 at 570 nm. Protein expression was induced by the addition of IPTG (final concentration of 10 μM), and the cells were incubated for an additional 3 h, after which they were harvested by centrifugation and suspended in 20 mL of 100 mM NaCl for sonication. The disrupted cells were centrifuged, resuspended in 12 mL of solubilization solution [20 mM Tris-HCl (pH 8.0) containing 7 M guanidine hydrochloride and 10 mM EDTA], and stirred for 2−3 h. DTT (final concentration of 0.1 M) was added and the solution stirred for 30 min to make the proteins, including RNase A, soluble. After the addition of 108 mL of 20 mM acetic acid, insoluble particles were removed by centrifugation, then the supernatant was dialyzed against 20 mM acetic acid. The resulting solution was mixed with 500 mL of refolding buffer [100 mM Tris-HOAc (pH 7.8) containing 0.1 M NaCl, 3.0 mM GSH, and 0.6 mM GSSG] and stirred for 48 h at 4 °C. To terminate the refolding reaction, the pH was lowered by adding 5 mL of acetic acid. The solution containing regenerated RNase A was concentrated with a Pellicon-2 ultrafiltration system (Millipore) equipped with a 3000 M_r cutoff membrane for purification.

Recombinant RNase A was purified in an FPLC apparatus (Pharmacia) equipped with a Mono S HR 5/5 column (7 mm × 54 mm, Pharmacia) equilibrated with 25 mM potassium phosphate buffer (pH 6.5). RNase A fractions were eluted with a linear gradient of 10 mM NaCl in the same buffer at a flow rate of 1.0 mL/min. The purified enzyme was diluted 1000-fold with water and then concentrated in a Centricon apparatus (Millipore).

Thermal and Pressure Unfolding Monitored by UV Spectroscopy. Absorption spectra between 270 and 310 nm were monitored at various temperatures or pressures with a modified Cary3 (Varian) absorption spectrometer as described elsewhere (*28*). The proteins (1 mg/mL) were dissolved in 50 mM MES buffer (pH 5.5). As its pK is relatively pressure and temperature independent (*41*), this buffer was used in both the heat- and pressure-induced unfolding experiments. Furthermore, thermal unfolding of the wild type and Phe46 mutants did not depend on pH in the range of 5.0−6.0 (data not shown). After each change in temperature or pressure, before spectral recording, the protein solution was incubated for 3 min to reach equilibration. The fourth derivation of the experimental spectra was obtained by the previously reported spectral shift method (*42*, *43*). All spectra were corrected for temperature- and pressure-dependent changes in water volume (*42*).

[1] Abbreviation: C>p, cytidine 2′,3′-cyclic monophosphate.

Table 1: Thermodynamic Parameters of RNase A and Its Phe46 Mutant Enzymes Calculated from Thermal Transition Curves at 0.1 MPa

enzyme	λ_N[a] (nm)	λ_D[b] (nm)	ΔH_m[c] (kJ/mol)	ΔS_m[d] (kJ mol^{-1} K^{-1})	T_m (°C)
wild type	286.2	284.4	431.4 ± 57.7	1.30 ± 0.18	58.0 ± 0.5
F46V	286.1	284.1	353.0 ± 23.6	1.10 ± 0.08	46.5 ± 0.2
F46E	285.2	284.0	255.0 ± 71.1	0.85 ± 0.20	26.4 ± 1.0
F46K	285.1	283.6	203.3 ± 32.5	0.69 ± 0.10	23.7 ± 0.8

[a] Wavelength at the highest peak between the two isosbestic points in the fourth-derivative spectra of enzymes in the native state. [b] Wavelength at the highest peak between the two isosbestic points in the fourth-derivative spectra of enzymes in the unfolded state. [c] Enthalpy change in thermally induced unfolding at T_m. [d] Entropy change in thermally induced unfolding at T_m.

Differential Scanning Calorimetry. DSC experiments were carried out in a VP-DSC microcalorimeter (MicroCal Inc.) at a scan rate of 0.5 °C/min. This was sufficient for the equilibration of thermal unfolding of the proteins that were analyzed. The proteins (1.0 mg/mL) were dissolved in 10 mM sodium acetate buffer (pH 5.5) containing 100 mM KCl and dialyzed against the same buffer overnight. After dialysis, the internal protein solution and external buffer were used as the sample and reference solutions, respectively. Heating curves were corrected by subtracting the baseline obtained with the reference solution. Reversibility was checked by continuous scanning of both the heating and cooling processes. The ORIGIN program (version 4.0, MicroCal Inc.) was used to analyze the scanned data.

CD Spectroscopy. CD spectra were recorded at 6.8 °C from 195 to 250 nm in a Jasco J720 spectropolarimeter with a 0.5 mm long optical path. The protein concentration was 20 μM in 50 mM MES buffer (pH 5.5). Baseline-corrected CD spectra were deconvoluted with the CDFIT program (*44*).

Steady State Kinetics. By monitoring the increase in A_{296} ($\Delta\epsilon_{296}$ was taken to be 516.4 M^{-1} cm^{-1}) (*46*), we assayed the hydrolytic activities of wild-type RNase A and its variant forms at 0.1 MPa and 20.0 °C against 0.2−6.0 mM C>p (*45*) in 0.2 M sodium acetate buffer (pH 5.5), conditions under which no thermal unfolding of the wild-type enzyme or its variants occurs.

RESULTS

Expression and Purification of Phe46 Mutant RNase A. An approximately 4.5 g (wet weight) *E. coli* pellet was obtained from 1 L of culture medium. SDS−PAGE confirmed the expression of three mutant enzymes. The attempt to purify a fourth mutant, F46A, was not successful because it was not adsorbed on the mono-S column during the last purification step, evidence that F46A could not fold to the correct conformation. We therefore assayed only the first three mutants. After the final purification step, their samples produced single bands on SDS−PAGE, the final yields being 20 mg of protein for F46V and 10 mg each for F46E and F46K.

Fourth-Derivative UV Spectra in Thermal and Pressure Unfolding. The fourth-derivative spectra exhibited sharp peaks between 280 and 290 nm, due to absorbance of the six tyrosine residues (*42*, *43*). Maximum peak wavelengths of the native state, λ_N, of the wild-type and F46V RNase A were very similar, whereas those of F46E and F46K RNase A were slightly blue-shifted (Tables 1 and 2), indicative of minor conformational differences in the wild-type, F46E, and F46K enzymes.

Table 2: Thermodynamic Parameters Calculated from Pressure Transition Curves at Various Temperatures

temp (°C)	λ_N (nm)	λ_D (nm)	ΔV[a] (mL/mol)	P_m (MPa)	ΔG_p[b] (kJ/mol)
			Wild Type		
40.0	286.0	nd[c]	−56.8 ± 10.1	617 ± 36	35.1 ± 3.0
48.0			−46.6 ± 3.5	425 ± 7	19.8 ± 1.1
50.0			−41.6 ± 2.9	430 ± 8	17.9 ± 0.9
55.0			−28.2 ± 4.2	312 ± 16	8.8 ± 0.8
			F46V		
32.1	285.9	284.0	−45.8 ± 3.4	262 ± 2	12.0 ± 0.8
36.6			−41.4 ± 5.9	220 ± 0	9.1 ± 1.3
37.0			−43.8 ± 3.6	196 ± 1	8.6 ± 0.8
40.0			−41.1 ± 3.5	182 ± 2	7.5 ± 0.7
			F46E		
4.0	285.1	283.3	−72.9 ± 9.5	167 ± 2	12.2 ± 1.7
9.0			−80.3 ± 7.1	158 ± 0	12.7 ± 1.1
10.0			−79.6 ± 7.3	162 ± 2	12.9 ± 1.4
20.0			−62.7 ± 3.3	88 ± 1	5.5 ± 0.4
			F46K		
3.5	284.8	283.6	−85.1 ± 9.9	100 ± 0	8.5 ± 1.0
5.7			−63.6 ± 6.1	116 ± 2	7.3 ± 0.9
6.0			−67.4 ± 11.7	128 ± 2	8.7 ± 1.3
8.7			−76.0 ± 13.4	103 ± 2	7.8 ± 1.6
10.0			−70.7 ± 2.3	96 ± 0	6.8 ± 0.2

[a] Volume change upon pressure-induced unfolding. [b] Change in Gibbs free energy upon pressure-induced unfolding at the measured temperature and 0.1 MPa. [c] Not determined.

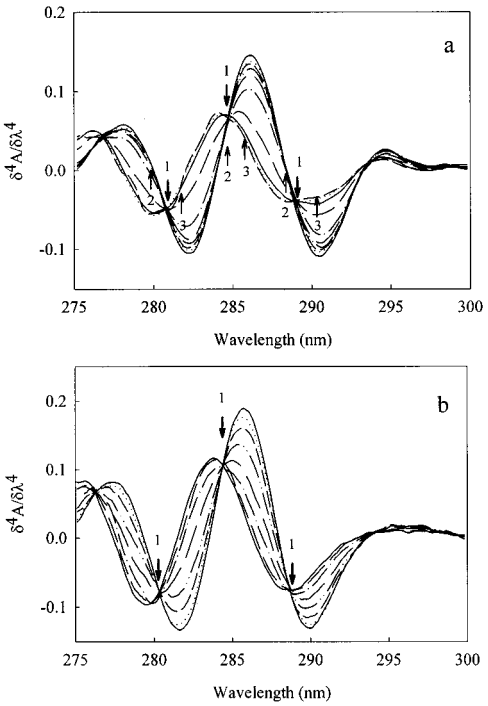

FIGURE 1: (a) Heat- and (b) pressure-induced unfolding of F46V RNase A. The major peak of the fourth-derivative UV spectra is blue-shifted as temperature or pressure increases. Arrows indicate the major (1) and minor (2 and 3) isosbestic points.

As the temperature or pressure was increased, the fourth-derivative bands of the wild-type and mutant enzymes shifted to blue, evidence of increased polarity in the environment of the tyrosine residues. This spectral shift produced three, clear, major isosbestic points at ~282, ~285, and ~288 nm (Figure 1) as was previously reported (*26*). Thermally

induced unfolding gave two additional minor isosbestic points beside each of the three major ones, for all enzymes, whereas pressure-induced unfolding yielded none. The minor isosbestic points present in thermally induced unfolding were due to the intrinsic temperature-dependent change in the tyrosine spectrum, as also found in the control experiments (*28*). Pressure-induced unfolding did not produce minor isosbestic points because the intrinsic spectrum of tyrosine is almost pressure insensitive (*28*). Collectively, these findings indicate that both heat- and pressure-induced unfolding are two-state transitions. Moreover, the maximum peak wavelength in the denatured state, λ_D, was identical (within the precision of our measurements) for the wild-type and mutant enzymes in the range of 283.3−284.4 nm in both the thermal and pressure unfolding experiments (Tables 1 and 2). This suggests that in the unfolded state tyrosine residues of both the wild-type and variant proteins are similarly exposed to water.

Unfolding by Heat. Plots of the $\partial^4A/\partial\lambda^4$ amplitude against temperature gave two-state, sigmoidal curves at each wavelength for each protein. The amplitude of $\partial^4A/\partial\lambda^4$ at λ_N, at which the largest change was observed, was used to fit the plots, utilizing eq 1 and fixing the change in heat capacity (ΔC_p) at 5.3 kJ/mol (*47*, *48*):

$$A = \frac{A_n - mT - (A_d - qT)}{1 + e^{-(\{\Delta H_m(1 - T/T_m) - \Delta C_p[T_m - T + T\ln(T/T_m)]\}/RT)}} + A_d - qT \quad (1)$$

where A, A_n, A_d, and ΔH_m are the observed amplitude of $\partial^4A/\partial\lambda^4$, the fitted amplitude of $\partial^4A/\partial\lambda^4$ in the native state, the fitted amplitude of $\partial^4A/\partial\lambda^4$ in the denatured state, and the enthalpy change in unfolding at T_m, respectively, and m and q are the correction factors reflecting the sloping baseline due to intrinsic changes in the tyrosine spectrum as a function of temperature. As a result, a very good correlation coefficient value, in excess of 0.999, was obtained in all cases.

The resulting energy parameters are shown in Table 1. T_m decreased from 46.5 to 23.7 °C in the following order: F46V > F46E > F46K. Clearly, these decreases in thermal stability were caused by the decrease in the enthalpy change. It is particularly noteworthy that replacement of phenylalanine with a charged group (F46E and F46K) markedly lowered thermal stability.

Unfolding at High Pressure. All the enzymes exhibited reversible pressure unfolding, but a larger kinetic hysteresis occurred during refolding when pressure rather than temperature was decreased. This agrees with previous findings (*37*, *49*). Each plot of $\partial^4A/\partial\lambda^4$ at λ_N against pressure produced a sigmoidal curve. Because the intrinsic tyrosine spectrum is nearly pressure independent, the plots obtained were fitted to eq 2 without introducing the m or q factor:

$$A = \frac{A_n - A_d}{1 + e^{-[(\Delta G_p + P\Delta V)/RT]}} + A_d \quad (2)$$

where ΔG_p and ΔV are the Gibbs free energy change at the experimental temperature and 0.1 MPa and the volume change, respectively (*50*). It should be noted that the true ΔG_p values may be smaller because we did not take into account the compressibility factor $\Delta\beta$ (*51*). Because we cannot access this parameter by our technique, we preferred to neglect the possible pressure dependence of ΔV. Furthermore, in all cases fitting produced a very good correlation coefficient (in excess of 0.999). Because T_m values for the wild type and its three variants were very different (Table 1), the pressure unfolding of each enzyme was monitored at various temperatures below their T_m values (Table 2).

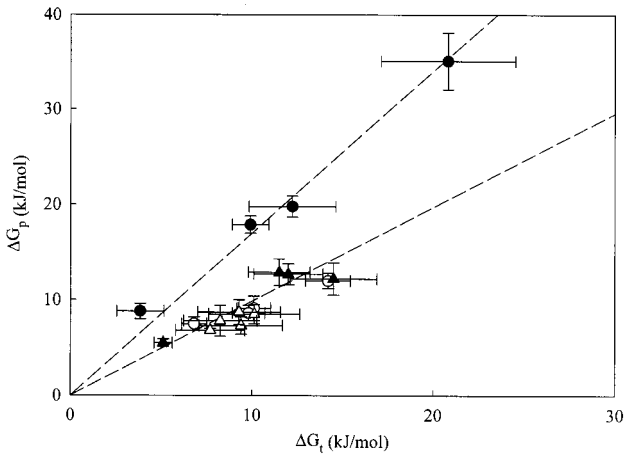

FIGURE 2: Correlation between free energy changes in heat-induced (ΔG_t) and pressure-induced (ΔG_p) unfolding of wild-type RNase A and three Phe46 mutants. ΔG_p was measured at various temperatures: 40.0, 48.0, 50.0, and 55.0 °C for the wild type (●), 32.1, 36.6, 37.0, and 40.0 °C for F46V (○), 4.0, 9.0, 10.0, and 20.0 °C for F46E (▲), and 3.5, 5.7, 6.0, 8.7, and 10.0 °C for F46K (△). For each enzyme, ΔG_t was calculated at each temperature from the curve-fitted, thermal unfolding curve. Straight lines show the linear relationship between ΔG_p and ΔG_p; the slope r equals 1.7 for the wild type and 0.92 for the mutants.

Comparison of Gibbs Free Energies in Temperature- and Pressure-Induced Unfolding. ΔG_t was determined from eq 3 at the temperatures at which pressure-induced unfolding experiments were conducted:

$$\Delta G_t = \Delta H_m(1 - T/T_m) - \Delta C_p[T_m - T + T\ln(T/T_m)] \quad (3)$$

ΔG_p values plotted as a function of ΔG_t at various temperatures gave a linear correlation for all the enzymes (Figure 2). r ($=\Delta G_p/\Delta G_t$) was 1.7 for the wild-type RNase A and 0.92 ± 0.03 for the mutants. As noted, the absolute value of r might be affected if $\Delta\beta$ is taken into account, but the compressibility of the mutants is assumed not to vary much from that of the wild type. Even if our determination of r has only relative significance, the reduction of r by a factor of nearly 2 indicates that the unfolding mechanism for the mutants differs from that for the wild-type RNase A.

ΔV, P_m, ΔG_p, and the expansibility, $\Delta\alpha$ [i.e., $\Delta\alpha = (\partial\Delta V/\partial T)_P = -(\partial\Delta S/\partial P)_T$], at 40.0 °C (wild type and F46V) and 10.0 °C (F46E and F46K) were determined from the representation of ΔG_p as a function of temperature and pressure. Three-dimensional curve fitting of this plot with the equation reported by Hawley (*52*) gave the parameters in Table 3. The results show that for all the mutants, as well as the wild-type RNase A enzyme, P_m decreases as the temperature increases. Wild-type RNase A was the most stable against pressure, stability against high pressure and heat decreasing in the following order: wild type > F46V > F46E > F46K. The change in volume, ΔV, was much more important for the wild type. As shown in Table 3, ΔV

Table 3: Thermodynamic Parameters of Wild-Type and Phe46 Mutant RNase A Calculated from Pressure Transition Curves at 40 or 10 °C

enzyme	standard temperature (°C)	ΔV (mL/mol)	P_m (MPa)	ΔG_p[a] (kJ/mol)	$\Delta V_{25°C}$[b] (mL/mol)	$\Delta\alpha$[c] (mL mol^{-1} K^{-1})
wild type	40.0	-58.6 ± 2.3	593 ± 7	34.8 ± 1.0	-86.5 ± 5.9	1.86 ± 0.24
F46V	40.0	-40.9 ± 0.7	174 ± 4	7.1 ± 0.3	-49.8 ± 3.1	0.59 ± 0.16
F46E	10.0	-74.5 ± 1.4	154 ± 1	11.5 ± 0.3	-62.0 ± 2.1	0.83 ± 0.23
F46K	10.0	-69.3 ± 4.4	102 ± 9	7.1 ± 1.0	-54.2 ± 12.4	1.01 ± 1.12

[a] Gibbs free energy change upon pressure-induced unfolding at the standard temperature and 0.1 MPa. [b] Volume change upon pressure-induced unfolding at 25 °C, calculated from the three-dimensional fitted curves. [c] Expansibility upon pressure-induced unfolding, calculated from the three-dimensional fitted curves.

Table 4: Thermodynamic Parameters of Wild-Type and Phe46 Mutant RNase A, Calculated from DSC Curves

enzyme	T_m (°C)	ΔH_{cal}[a] (kJ/mol)	CU[b]	CU_{2nd}[c]
wild type	60.7	449.0	1.00	1.01
F46V	46.8	353.1	1.00	1.05
F46E	32.0	225.1	1.10	1.22
F46K	24.3	242.7	1.10	1.17

[a] Enthalpy change upon thermally induced unfolding, calculated from the observed DSC curves. [b] $CU = \Delta H_{cal}/\Delta H_{eff}$, where ΔH_{eff} is the van't Hoff enthalpy. [c] CU values calculated with ΔH_{cal} from DSC curves obtained by reheating.

values for the wild type and F46V could be compared directly at 40 °C. For the two other mutants, ΔV values could be determined only at low temperatures, at which the wild type was too stable for determination of its ΔV. The comparison therefore was made at 25 °C by extrapolation of the fitted function according to Hawley (*52*). The smaller absolute values of ΔV for the mutants versus the wild type are evidence of different unfolding mechanisms. $\Delta\alpha$ values were positive for all the enzymes, consistent with a previous report, in which the thermal expansibility of the unfolded state was thought to be larger than that of the folded state (*53*). Moreover, $\Delta\alpha$ values for the mutants were significantly smaller than the value for the wild type. Although the reason for the difference in this parameter is not clear, its decrease supports the probable existence of a partially ordered structure in the unfolded state.

DSC Study of Wild-Type RNase A and Its Mutant Enzymes. The thermal unfolding processes of the wild-type, F46V, F46E, and F46K enzymes obtained by DSC were completely reversible. The calorimetric enthalpy at T_m (ΔH_{cal}) and T_m values, determined from plots of molar heat capacity (C_p) as a function of temperature, are shown in Table 4. They are very similar to the values deduced from the fourth-derivative UV spectroscopic analysis (Tables 1 and 4). This suggests that the global protein conformation unfolds cooperatively, but whereas the wild-type and F46V proteins have a ΔH_{cal} to van't Hoff enthalpy ratio (CU) of nearly 1.00, indicative of two-state unfolding, the value for F46E and F46K is 1.1 (Table 4). Deconvolution of the DSC curves of F46E and F46K shows two separate adjacent peaks (Figure 3) which suggest three-state unfolding with a transient intermediate. Moreover, the second CU value (CU_{2nd}) of F46V is slightly larger than 1.00 (1.05), evidence that the unfolding of F46V also proceeds via an intermediate. These findings indicate a loss of cooperativity in thermal unfolding of the Phe46 mutants. This noncooperativity could not be detected by fourth-derivative UV spectral analysis.

Change in the Secondary Structures of Phe46 Mutants. CD spectra from 195 to 250 nm of wild-type and F46V RNase A were very similar, evidence of no difference in secondary structure. In contrast, the CD spectra of F46E and F46K indicate slight changes in secondary structure with respect to wild-type RNase A. Their spectral minima are blue-shifted, and in F46K, the amplitude of the spectrum is decreased (Figure 4). Structural components analyzed by deconvolution of the measured spectra gave an R value of 14%. This shows that F46E and F46K RNase A have decreased β-sheet and increased random coil contents, more pronounced for F46K than for F46E (Table 5).

The secondary structure estimation program of the PSA server (*54*−*56*) showed that the decreases in β-sheet content and increases in random coil content of F46E and F46K occur only around the mutated position (Figure 5). This suggests that residues 44−50 change from a β-sheet to a random coil as a result of the replacement of Phe46 with glutamic acid or lysine.

Steady State Kinetic Parameters. As shown in Table 6, the K_m and k_{cat} values of the wild type and mutants are not markedly affected by the replacement of Phe46. For F46V, K_m and k_{cat} are only slightly affected (by approximately 1.6 kJ/mol) in both their substrate binding and catalytic reactions, as determined by the equations $-RT \ln[(k_{cat}$ of F46V)/(k_{cat} of wild type)] and $-RT \ln[(K_m$ of wild type)/(K_m of F46V)]. The K_m of F46E is very similar to that of F46V, whereas its k_{cat} is smaller by approximately 2.0 kJ/mol. Of the three mutants, the k_{cat} and K_m values of F46K were the most affected, being increased by 4.1 and 4.7 kJ/mol, respectively, compared to the wild-type values. Such changes in the kinetic parameters of F46E and F46K are, however, too small to be attributed to marked conformational destruction of the active site structure. For example, a very marked decrease in k_{cat}, corresponding to 6.1 kJ/mol, has been reported for the Phe120 mutant RNase A (*57*), but its crystal structure shows only a small (∼1 Å) positional change at His119.

DISCUSSION

Importance of Hydrophobic Interactions of Phe46 in Maintaining the Conformational Stability of RNase A. Val, Glu, or Lys substitution for Phe46 markedly decreased the conformational stability of RNase A with respect to heat and pressure. Moreover, CD analysis showed that when Phe46 was replaced with ionic residues, even the folded state conformation was perturbed. These effects are attributed to the loss of hydrophobic interaction with other residues. In the case of F46V, the folded state structure appears to be relatively unchanged. Due to amino acid replacement, changes in cavity volume and area and in Gibbs free energy are linearly correlated by approximately 100−140 J mol^{-1} Å^{-3} and 85 J mol^{-1} Å^{-2}, respectively (*58*). Loss of Gibbs

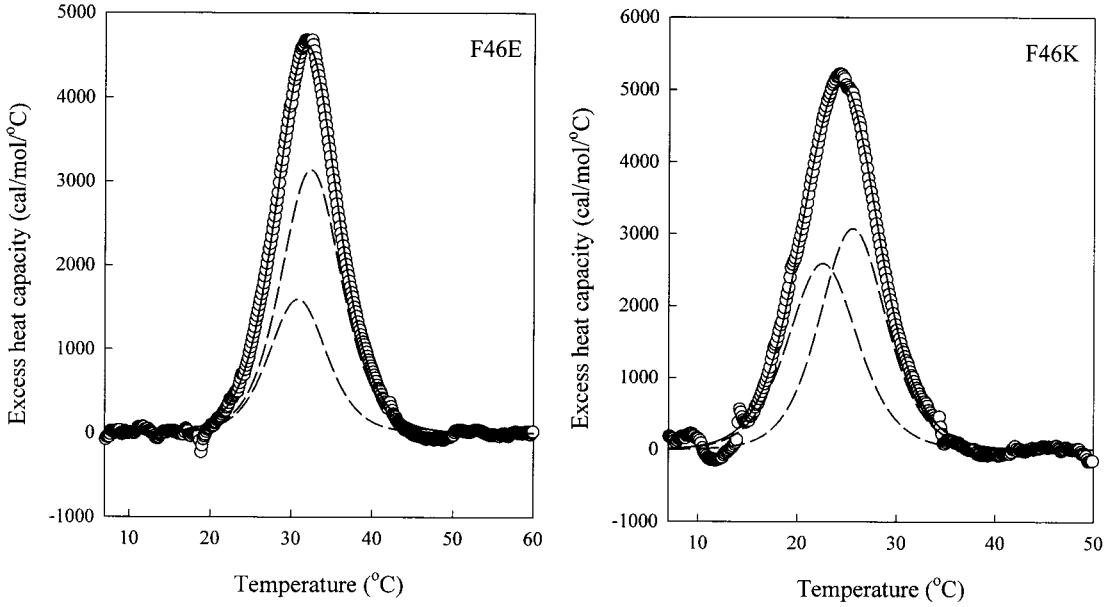

FIGURE 3: Deconvolution of F46E (left) and F46K (right) DSC profiles. The proteins were dissolved in 10 mM sodium acetate buffer (pH 5.5) containing 100 mM KCl: (—) fitted curves and (– – –) deconvoluted curves.

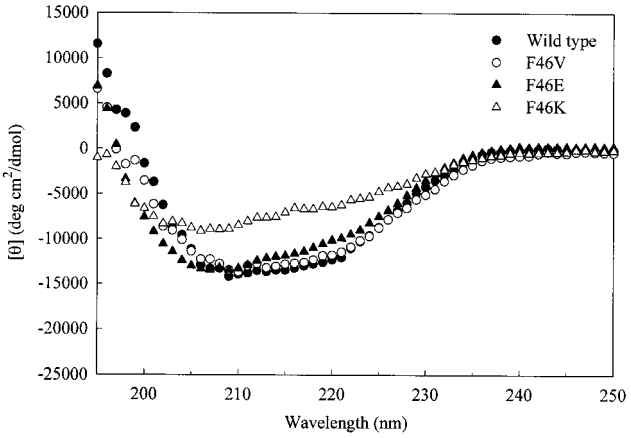

FIGURE 4: Far-UV CD spectra of wild-type RNase A and Phe46 mutants. Component analysis of the secondary structure with the CDFIT program is shown in Table 5.

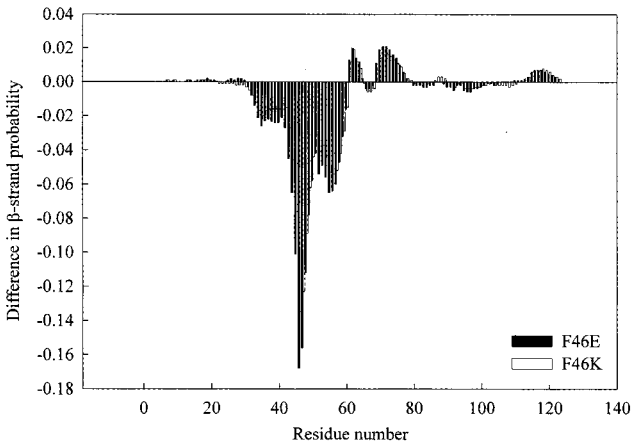

FIGURE 5: Location of lost β-sheet structures in F46E and F46K mutant RNase A, estimated by the PSA server. The β-strand probabilities of F46E and F46K are subtracted from the probability of wild-type RNase A, and plotted against each of the 124 amino acid residues of RNase A.

Table 5: Structural Elements of Wild-Type and Phe46 Mutant RNase A, Estimated with the CDFIT Program

enzyme	% α-helix	% β-sheet	% random coil
wild type	33	27	40
F46V	26	30	44
F46E	36	14	50
F46K	29	16	55

Table 6: Kinetic Parameters for C>p in Wild-Type and Phe46 Mutant RNase A[a]

enzyme	k_{cat} (s^{-1})	K_m (mM)	k_{cat}/K_m (mM^{-1} s^{-1})
wild type	2.68 ± 0.04	0.37 ± 0.02	7.24 ± 0.27
F46V	1.37 ± 0.10	0.69 ± 0.19	1.99 ± 0.32
F46E	0.62 ± 0.03	0.61 ± 0.19	1.02 ± 0.21
F46K	0.50 ± 0.03	2.58 ± 0.30	0.19 ± 0.04

[a] All measurements taken at 20 °C.

free energy for F46V in the thermal unfolding experiments was 700 J mol^{-1} $Å^{-3}$ and 400 J mol^{-1} $Å^{-2}$. These large energy values suggest that π-electron interactions, in addition to hydrophobic ones, contribute to conformational stability, as does the Phe31 of protein P2 which is reported to be a key residue for stabilization of the hydrophobic core of P2 (*50*, *59*, *60*). The importance of hydrophobic interactions at position 46 also is supported by the fact that F46A RNase A, in which hydrophobic interaction at that position is greatly weakened, no longer can fold to the native state. It is surprising to find such strong stability dependence on hydrophobic interactions at a single amino acid residue. In this respect, RNase A is comparable to the 98-amino acid protein acylphosphatase, in which three hydrophobic residues with long-range interactions are required for formation of the folding transition state (*61*). We propose that in RNase A, Phe46 serves as an analogue of one of the key residues.

Thermodynamics of Heat- and Pressure-Induced Unfolding. Substitution of valine, glutamic acid, or lysine for Phe46 not only dramatically lowered the T_m and P_m values but also lowered the $\Delta G_p/\Delta G_t$ ratio by a factor of nearly 2. This can be explained only by a modified unfolding mechanism. Interestingly, Torrent et al. found that replacement of CFIS

residues (Ile106, Ile107, Val108, Ala109, Val116, and Val118) with a smaller hydrophobic residue markedly lowered T_m and P_m values but did not affect the $\Delta G_p/\Delta G_t$ relationship (*28*). Phe46 therefore appears to be essential for the stability of RNase A.

Structural Characterization of the Folded and Unfolded States. Decreases in the stabilities of the Phe46 mutants may be due to structural changes in the folded or unfolded state. CD analysis found limited conformational modification for the folded state of F46E and F46K but not for the F46V mutant. Furthermore, the three mutants remained catalytically active, but to a lesser degree than the wild-type RNase A. These findings suggest relatively small structural changes occur in the mutants in the folded state, which would only partly account for their decreased stabilities. Indeed, decreased stability also may be caused by structural changes in the mutants in the unfolded state. For a better understanding, consider the unfolded states. From UV analysis, we know that ΔG_p and ΔG_t in the unfolding reaction of the wild type are very different ($r = 1.7$), an indication that under heat- and pressure-induced unfolding the structures of the unfolded states are not the same. The situation differs for the three mutants; not only is thermal stability reduced, stability versus pressure is even more reduced, resulting in an r value of $\sim$1. This suggests that in the mutants heat and pressure produce a similarly structured unfolded state. What are the structural features of this state? DSC analysis showed a two-step unfolding process indicative of the presence of a partially unfolded state prior to full unfolding. The unfolded state detected by the fourth-derivative UV spectra probably reflects this intermediate state, which would explain the lowered stability of the mutants, the markedly decreased ΔG_p values, and the decreased absolute ΔV values. Conceivably, the unfolding intermediate corresponds to the hydrophobic core, or part of it. In RNase A, however, the six Tyr residues are in the surface region of the protein. It is therefore understandable that the fourth-derivative UV spectra technique cannot discriminate between the unfolding intermediate and the fully unfolded structure.

Structural Model. Our findings led us to propose a structural model. The single hydrophobic core of RNase A is divided into two parts, A and B. The smaller part, A, is composed of Met29, Met30, Leu35, and Phe46 and the larger part, B, of Ala4, Ala5, Ala6, Phe8, Met13, Val47, Ala52, Val54, Ala56, Val57, Val63, Met79, Ile81, Ala102, Ile106, Ile107, Val108, Ala109, Val116, Pro117, Val118, Phe120, Ala122, and Val124 (Figure 6). The first β-sheet (residues 43−48), located at the boundary of the two parts, appears to link them, producing a single hydrophobic core. Parts A and B have similar conformational stabilities and unfold under the same energy conditions. When a charged group is introduced at position 46, local change to a random coil occurs at the first β-sheet (based on CD analysis results and the PSA server). The conformation of part B, which consists of all the substrate binding sites and catalytic residues that participate in the hydrolysis of C>p, appears to be unchanged on the basis of kinetic analysis findings. This suggests that the mutation of Phe46 to other amino acid residues destabilizes A, but not B, leading to loss of unfolding cooperativity in the hydrophobic core. Because parts A and B in the mutant enzymes have different stabilities, the unfolding intermediate can be distinguished.

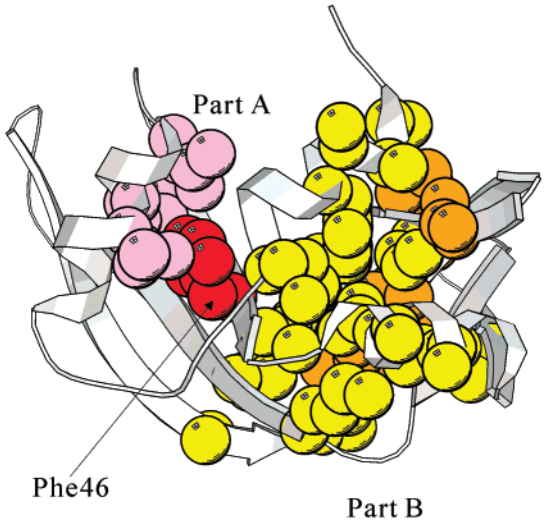

FIGURE 6: Structure of the hydrophobic core of RNase A. This figure was drawn with MOLSCRIPT (*63*). The backbone is shown as a gray ribbon. Colored CPK balls (pink, red, yellow, and gold) represent the side chains of hydrophobic residues which make up the single hydrophobic core. The smaller part of the core, composed of Met29, Met30 (pink), and Phe46 (red), constitutes part A. The remaining portion, shown in yellow and gold (CFIS residues Ile106, Ile107, Val108, Ala109, Val116, and Val118 are gold), constitutes part B.

Predicted Role of Phe46 in Folding. Phe46 contributes to the construction of the hydrophobic core which is essential both for stabilizing the conformation and producing the correct RNase A conformation, as shown by the F46E and F46K mutants. This is explained by the hydrophobic interaction of Phe46 with nearby hydrophobic residues of part A, an interaction essential for formation of the first β-sheet. Indeed, mutational manipulation of the hydrophobic core of a protein can change the α-helix in the secondary structure to a β-sheet (*62*). In our model, during the unfolding of the mutants, part A uncoils before part B, indicating that its structure (which bears Phe46 in the wild type) is indispensable during the early steps of chain folding. Phe46 appears to act as a CFIS essential for promoting correct folding.

ACKNOWLEDGMENT

We thank Mr. Christian Valentin for his expert technical assistance in the high-pressure experiments.

REFERENCES

1. Raines, R. T. (1998) *Chem. Rev. 98*, 1045−1066.
2. Cuchillo, C. M., Vilanova, M., and Nogues, M. V. (1997) in *Ribonucleases: Structures and Functions* (D'Alessio, G., and Riordan, J. F., Eds.) pp 271−300, Academic Press, New York.
3. Sendak, R. A., Rothwarf, D. M., Wedemeyer, W. J., Houry, W. A., and Scheraga, H. A. (1996) *Biochemistry 35*, 12978−12992.
4. Schmid, F. X. (1982) *Eur. J. Biochem. 128*, 77−80.
5. Dodge, R. W., Laity, J. H., Rothwarf, D. M., Shimotakahara, S., and Scheraga, H. A. (1994) *J. Protein Chem. 13*, 409−421.
6. Houry, W. A., Rothwarf, D. M., and Scheraga, H. A. (1994) *Biochemistry 33*, 2516−2530.
7. Houry, W. A., Rothwarf, D. M., and Scheraga, H. A. (1995) *Nat. Struct. Biol. 2*, 495−503.
8. Houry, W. A., Rothwarf, D. M., and Scheraga, H. A. (1996) *Biochemistry 35*, 10125−10133.
9. Houry, W. A., and Scheraga, H. A. (1996) *Biochemistry 35*, 11734−11746.

10. Shimotakahara, S., Rios, C. B., Laity, J. H., Zimmerman, D. E., Scheraga, H. A., and Montelione, G. T. (1997) *Biochemistry 36*, 6915−6929.
11. Laity, J. H., Lester, C. C., Shimotakahara, S., Zimmerman, D. E., Montelione, G. T., and Scheraga, H. A. (1997) *Biochemistry 36*, 12683−12699.
12. Lester, C. C., Xu, X., Laity, J. H., Shimotakahara, S., and Scheraga, H. A. (1997) *Biochemistry 36*, 13068−13076.
13. Iwaoka, M., Juminaga, D., and Scheraga, H. A. (1998) *Biochemistry 37*, 4490−4501.
14. Dodge, R. W., and Scheraga, H. A. (1996) *Biochemistry 35*, 1548−1559.
15. Juminaga, D., Wedemeyer, W. J., and Scheraga, H. A. (1998) *Biochemistry 37*, 11614−11620.
16. Li, Y. J., Rothwarf, D. M., and Scheraga, H. A. (1995) *Nat. Struct. Biol. 2*, 489−494.
17. Xu, X., Rothwarf, D. M., and Scheraga, H. A. (1996) *Biochemistry 35*, 6406−6417.
18. Rothwarf, D. M., Li, Y. J., and Scheraga, H. A. (1998) *Biochemistry 37*, 3760−3766.
19. Rothwarf, D. M., Li, Y. J., and Scheraga, H. A. (1998) *Biochemistry 37*, 3767−3776.
20. Nemethy, G., and Scheraga, H. A. (1979) *Proc. Natl. Acad. Sci. U.S.A. 76*, 6050−6054.
21. Gutte, B. (1977) *J. Biol. Chem. 252*, 663−670.
22. Haas, E., Montelione, G. T., McWherter, C. A., and Scheraga, H. A. (1987) *Biochemistry 26*, 1672−1683.
23. Beals, J. M., Haas, E., Krausz, S., and Scheraga, H. A. (1991) *Biochemistry 30*, 7680−7692.
24. Talluri, S., Falcomer, C. M., and Scheraga, H. A. (1993) *J. Am. Chem. Soc. 115*, 3041−3047.
25. Taniuchi, H. (1970) *J. Biol. Chem. 245*, 5459−5468.
26. Fujii, T., Doi, Y., Ueno, H., and Hayashi, R. (2000) *J. Biochem. 127*, 877−881.
27. Coll, M. G., Protasevich, I. I., Torrent, J., Ribo, M., Lobachov, V. M., Makarov, A. A., and Vilanova, M. (1999) *Biochem. Biophys. Res. Commun. 265*, 356−360.
28. Torrent, J., Connelly, J. P., Coll, M. G., Ribo, M., Lange, R., and Vilanova, M. (1999) *Biochemistry 38*, 15952−15961.
29. Torrent, J., Rubens, P., Ribo, M., Heremans, K., and Vilanova, M. (2001) *Protein Sci. 10*, 725−734.
30. Morgan, C. J., Miranker, A., and Dobson, C. M. (1998) *Biochemistry 37*, 8473−8480.
31. Qi, P. X., Sosnick, T. R., and Englander, S. W. (1998) *Nat. Struct. Biol. 5*, 882−884.
32. Jennings, P. A. (1998) *Nat. Struct. Biol. 5*, 846−848.
33. Morild, E. (1981) *Adv. Protein Chem. 34*, 93−166.
34. Gross, M., and Jaenicke, R. (1994) *Eur. J. Biochem. 221*, 617−630.
35. Heremans, K., and Smeller, L. (1998) *Biochim. Biophys. Acta 1386*, 353−370.
36. Ruan, K., and Weber, G. (1993) *Biochemistry 32*, 6295−6301.
37. Panick, G., and Winter, R. (2000) *Biochemistry 39*, 1862−1869.
38. Bryngelson, J. D., Onuchic, J. N., Socci, N. D., and Wolynes, P. G. (1995) *Proteins 21*, 167−195.
39. Dumoulin, M., Ueno, H., Hayahsi, R., and Balny, C. (1999) *Eur. J. Biochem. 262*, 475−483.
40. Chatani, E., Tanimizu, N., Ueno, H., and Hayashi, R. (2001) *J. Biochem. 129*, 917−922.
41. Fukada, H., and Takahashi, K. (1998) *Proteins 33*, 159−166.
42. Lange, R., Frank, J., Saldana, J. L., and Balny, C. (1996) *Eur. Biophys. J. 24*, 277−283.
43. Lange, R., Bec, N., Mozhaev, V. V., and Frank, J. (1996) *Eur. Biophys. J. 24*, 284−292.
44. Greenfield, N., and Fasman, G. D. (1969) *Biochemistry 8*, 4108−4116.
45. Moussaoui, M., Nogues, M., Guasch, A., Barman, T., Travers, F., and Cuchillo, C. (1998) *J. Biol. Chem. 273*, 25565−25572.
46. Boix, E., Nogues, M. V., Schein, C. H., Benner, S. A., and Cuchillo, C. M. (1994) *J. Biol. Chem. 269*, 2529−2534.
47. Makhatadze, G. I., and Privalov, P. L. (1995) *Adv. Protein Chem. 47*, 307−425.
48. Yamaguchi, T., Yamada, H., and Akasaka, K. (1995) *J. Mol. Biol. 250*, 689−694.
49. Takeda, N., Kato, M., and Taniguchi, Y. (1995) *Biochemistry 34*, 5980−5987.
50. Mombelli, E., Afshar, M., Fusi, P., Mariani, M., Tortora, P., Connelly, J. P., and Lange, R. (1997) *Biochemistry 36*, 8733−8742.
51. Prehoda, K. E., Mooberry, E. S., and Markley, J. L. (1998) *Biochemistry 37*, 5785−5790.
52. Hawley, S. A. (1971) *Biochemistry 10*, 2436−2442.
53. Panick, G., Vidugiris, G. J., Malessa, R., Rapp, G., Winter, R., and Royer, C. A. (1999) *Biochemistry 38*, 4157−4164.
54. Stultz, C. M., White, J. V., and Smith, T. F. (1993) *Protein Sci. 2*, 305−314.
55. Stultz, C. M., Nambudripad, R., Lathrop, R. H., and White, J. V. (1997) in *Advances in Molecular and Cell Biology* (Allewell, N., and Woodward, C., Eds.) pp 447−506, JAI Press, Greenwich, CT.
56. White, J. V., Stultz, C. M., and Smith, T. F. (1994) *Math. Biosci. 119*, 35−75.
57. Chatani, E., Hayashi, R., Moriyama, H., and Ueki, T. (2002) *Protein Sci. 11*, 72−81.
58. Eriksson, A. E., Baase, W. A., Zhang, X. J., Heinz, D. W., Blaber, M., Baldwin, E. P., and Matthews, B. W. (1992) *Science 255*, 178−183.
59. Fusi, P., Goossens, K., Consonni, R., Grisa, M., Puricelli, P., Vecchio, G., Vanoni, M., Zetta, L., Heremans, K., and Tortora, P. (1997) *Proteins 29*, 381−390.
60. Consonni, R., Santomo, L., Fusi, P., Tortora, P., and Zetta, L. (1999) *Biochemistry 38*, 12709−12717.
61. Vendruscolo, M., Paci, E., Dobson, C. M., and Karplus, M. (2001) *Nature 409*, 641−645.
62. Dalal, S., and Regan, L. (2000) *Protein Sci. 9*, 1651−1659.
63. Kraulis, P. (1991) *J. Appl. Crystallogr. 24*, 946−950.

BI011365E